Binuclear Palladium Complexes with Bridging Hydrides. Unusual Coordination Behavior of $LiBEt_4$ and $NaBEt_4$

Michael D. Fryzuk,* Brian R. Lloyd, Guy K. B. Clentsmith, and Steven J. Rettig†

Contribution from the Department of Chemistry, University of British Columbia, 2036 Main Mall, Vancouver, British Columbia, Canada V6T 1Z1

Received July 12, 1993⊛

Abstract: The reaction of $Pd(dippp)Cl_2$ (dippp = 1,3-bis(diisopropylphosphino)propane) with a 1:1 mixture of $LiBEt_2H_2$ and $LiBEt_4$ in THF generates the binuclear hydride derivative $[(dippp)Pd]_2(\mu\text{-}H)_2\cdot LiBEt_4$ (**1**) in which the $LiBEt_4$ is bound to the palladium hydride core. The bare palladium hydride dimer $[(dippp)Pd]_2(\mu\text{-}H)_2$ (**2**) was prepared by reaction of 2 equiv of $KBEt_3H$ in toluene with $Pd(dippp)I_2$. Addition of $LiBEt_4$ to the bare palladium dimer **2** generates the $LiBEt_4$ adduct **1**; this approach has been extended to the preparation of $[(dippp)Pd]_2(\mu\text{-}H)_2\cdot NaBEt_4$ (**3**) and $[(dippp)Pd]_2(\mu\text{-}H)_2\cdot LiAlEt_4$ (**4**) by the addition of $NaBEt_4$ and $LiAlEt_4$ respectively to **2**. On the basis of NMR spectroscopy, there is no evidence for dissociation of the lithium of sodium borate or aluminate salts from the hydride dimer but the $ME'Et_4$ (M = Li, Na; E' = B, Al) units are labile on the basis of exchange studies and variable temperature NMR data. Crystals of $[(dippp)Pd]_2(\mu\text{-}H)_2\cdot LiBEt_4\cdot 0.5(C_6H_{14})$ (**1**) are monoclinic, a = 11.537(2) Å, b = 19.114(2) Å, c = 24.020(1) Å, β = 98.674(9)°, Z = 4, space group $P2_1/n$; those of $[(dippp)Pd]_2(\mu\text{-}H)_2$ (**2**) are monoclinic, a = 13.128(1) Å, b = 14.362(4) Å, c = 20.353(1) Å, β = 99.593(6)°, Z = 4, space group $P2_1/n$; and those of $[(dippp)Pd]_2(\mu\text{-}H)_2\cdot NaBEt_4$ (**3**) are monoclinic, a = 20.099(2) Å, b = 11.457(5) Å, c = 21.600(3) Å, β = 92.87(1)°, Z = 4, space group $P2_1/c$. The structures were solved by the Patterson method and were refined by full-matrix least-squares procedures to R = 0.033, 0.052, and 0.033 (R_w = 0.029, 0.054, and 0.028) for 5954, 4560, and 5018 reflections with $I \geq 3\sigma(I)$, respectively. In the solid-state structure of **1**, there are three C–H···Li interactions from the ethyl groups attached to boron whereas in the solid-state structure of **3** there are four such C–H···Na interactions.

Introduction

The concept of metal basicity was introduced over twenty years ago by Shriver[1] and has since been updated by Werner.[2] In this formalism, a metal complex acts as a Lewis base and formally donates a pair of electrons to a Lewis acid. Although the idea can be applied to oxidative addition chemistry, wherein the Lewis acid component is an electrophilic species such as H^+, O_2, organic halides, or electron-deficient olefins such as tetracyanoethylene, it is also applicable to neutral Lewis acid acceptor molecules such as the group 13 derivatives, BF_3 and Al_2Me_6, and mercury halides. Some of the typical neutral Lewis acids that have been shown to interact with metal complexes are the following: Al_2Br_6 in $Co_2(CO)_8\cdot AlBr_3$;[3] $HgCl_2$ in a variety of complexes of the type $(\eta^5\text{-}C_5H_5)Co(CO)_2\cdot HgCl_2$ and $Fe(CO)_3(PPh_3)_2\cdot HgCl_2$; Al_2Me_6 in $(\eta^5\text{-}C_5H_5)_2WH_2\cdot AlMe_3$,[4] $(\eta^5\text{-}C_5H_5)_3ZrH\cdot AlMe_3$,[5] and $(\eta^5\text{-}C_5H_5)_2ReH\cdot AlMe_3$;[6] BF_3 in $(\eta^5\text{-}C_5H_5)_2WH_2\cdot BF_3$ and $(\eta^3\text{-}C_5H_5)_2ReH\cdot BF_3$;[7] and $Al_2Me_4Cl_2$ in $(\eta^4\text{-}C_5H_5)Rh(PMe_3)_2\cdot Al_2Me_4Cl_2$.[8] While this list is not comprehensive, it does focus on the main types of interactions possible; these are illustrated by the structures **A–D** below.

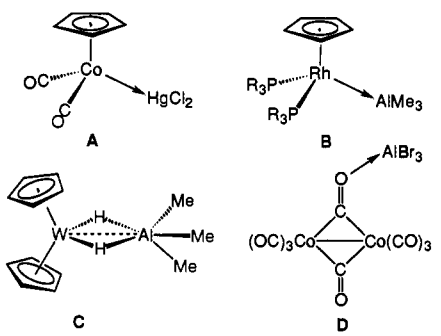

In general, the Lewis acid can be associated with the metal center density (cf. **A** and **B**) or with the ligands, generally the hydrides (cf. **C**) or the carbonyls (cf. **D**)[3]. For example, in $(\eta^5\text{-}C_5H_5)_2WH_2\cdot AlMe_3$ (**C**), the nature of the interaction of the $AlMe_3$ unit with $(\eta^5\text{-}C_5H_5)WH_2$ was only resolved with the aid of a low-temperature X-ray crystal structure. Formally d^0 metal complexes can also engage in interactions with Lewis acids as evidenced by recent work in which zirconium methyl and hydride derivatives generate cationic, base-free derivatives by reaction with $B(C_6F_5)_3$.[9,10]

Recently, we discovered a new type of complexation that uses a palladium dimer with bridging hydrides as the Lewis base and salts of the general formula $M^+ER_4^-$ (M = Li, Na; E = B, Al; R = alkyl) as the Lewis acids.[11] That alkali metal salts of group 13 "ate" compounds, such as $LiBEt_4$ and $LiAlEt_4$, could act as Lewis acids was unprecedented to our knowledge. Given the importance of Lewis acids in promoting reactions such as Ziegler–Natta polymerization of olefins, hydrocyanation of olefins,[12] dimerization of ethylene,[13] and migratory insertion reactions,[14] we began a systematic investigation of Lewis acid–Lewis base

† Professional Officer: UBC Crystallographic Service.

⊛ Abstract published in *Advance ACS Abstracts,* March 15, 1994.

(1) Shriver, D. F. *Acc. Chem. Res.* **1970**, *3*, 231.
(2) Werner, H. *Angew. Chem., Int. Ed. Engl.* **1983**, *22*, 927.
(3) Kristoff, J. S.; Shriver, D. F. *Inorg. Chem.* **1974**, *13*, 499.
(4) Bruno, J. W.; Huffman, J. C.; Caulton, K. G. *J. Am. Chem. Soc.* **1984**, *106*, 444.
(5) Kopf, J.; Vollmer, H.-J.; Kaminsky, W. *Cryst. Struct. Commun.* **1980**, *9*, 985.
(6) Brunner, H.; Wailes, P. C.; Kaesz, H. D. *J. Inorg. Nucl. Chem. Lett.* **1965**, *1*, 125.
(7) Johnson, M. P.; Shriver, D. F. *J. Am. Chem. Soc.* **1966**, *88*, 301.
(8) Mayer, J. M.; Calabrese, J. C. *Organometallics* **1984**, *3*, 1292.
(9) Yang, X.; Stern, C. L.; Marks, T. J. *J. Am. Chem. Soc.* **1991**, *113*, 3623.
(10) Yang, X.; Stern, C. L.; Marks, T. J. *Angew. Chem., Int. Ed. Engl.* **1992**, *31*, 1375.
(11) Fryzuk, M. D.; Lloyd, B. R.; Clentsmith, G. K. B.; Rettig, S. J. *J. Am. Chem. Soc.* **1991**, *113*, 4332.
(12) Parshall, G. W. *Homogeneous Catalysis*; Wiley-Interscience: New York, 1980.
(13) Fischer, K.; Jonas, K.; Misbach, P.; Stabba, R.; Wilke, G. *Angew. Chem., Int. Ed. Engl.* **1973**, *12*, 943.
(14) Butts, S. B.; Strauss, S. H.; Holt, E. M.; Stimson, R. E.; Alcock, N. W.; Shriver, D. F. *J. Am. Chem. Soc.* **1980**, *102*, 5093.

0002-7863/94/1516-3804$04.50/0

interactions using palladium hydride dimers and the simple alkali metal salts of peralkyl borates and aluminates. In this paper we report solid-state and solution structures of adducts of the general formula $[(dippp)Pd]_2(\mu\text{-}H)_2\cdot ME'Et_4$ (where dippp = 1,3-bis-(diisopropylphosphino)propane; M = Li or Na, E' = B or Al) as well as their relative stabilities. The solid-state structure of the parent palladium hydride dimer $[(dippp)Pd]_2(\mu\text{-}H)_2$ is also included.

Experimental Section

Procedures. Unless otherwise stated all manipulations were performed under an atmosphere of dry, oxygen-free dinitrogen or argon by means of standard Schlenk or glovebox techniques. The glovebox used was a Vacuum Atmospheres HE-553-2 device equipped with a MO-40-2H purification system and a –40 °C freezer. ^1H and $^{31}P\{^1H\}$ NMR spectroscopy were performed on a Varian XL-300 instrument operating at 300 MHz and 121.4 MHz, respectively. ^2D NMR spectroscopy was also performed on the Varian instrument operating at 46 MHz. $^1H\{^{31}P\}$ NMR spectroscopy was performed upon a Bruker AMX-500 instrument operating at 500.1 MHz. ^1H NMR spectra were referenced to internal C_6D_5H (7.15 ppm), $C_6D_5CD_2H$ (2.09 ppm), or $CHCl_3$ (7.24 ppm). ^{31}P NMR spectra were referenced to external $P(OMe)_3$ (141.0 ppm with respect to 85% H_3PO_4 at 0.0 ppm). Longitudinal relaxation times for the hydrides were measured by a standard inversion–recovery sequence supplied with Version 6.0c of the Varian VXR series software. Kinetic data were simulated by the DNMR-SIM program.[15]

Microanalyses (C, H, halogen) were performed by Mr. P. Borda of this department.

Materials. Dippp was prepared by a published procedure.[16] EtLi was prepared by a published procedure[17] and recrystallized from toluene. $LiAlEt_4$ and $LiBEt_4$ were prepared by adding $AlEt_3$ (Aldrich) or BEt_3 (Aldrich), respectively, to EtLi and recrystallized from toluene.[18] $NaBEt_4$ (Strem) was used as supplied. $KBEt_3H$ was prepared by addition of BEt_3 to a slurry of KH (BDH) in toluene and was recrystallized from toluene; $KBEt_3D$ was prepared likewise from KD.[19] $PdCl_2$ was obtained on loan from Johnson-Matthey and used to prepare $Pd(C_6H_5C{\equiv}N)_2Cl_2$.[20]

Hexanes, toluene, pentane, Et_2O, and THF were heated to reflux over CaH_2 prior to a final distillation from either sodium metal or sodium benzophenone ketyl under an Ar atmosphere. Acetone was dried over 4-Å sieves and sparged with dinitrogen. Deuterated solvents were dried by activated 3-Å molecular sieves; oxygen was removed by trap-to-trap distillation and 3 freeze–pump–thaw cycles.

Pd(dippp)Cl$_2$. To a solution of $Pd(C_6H_5C{\equiv}N)_2Cl_2$ (4.37 g; 11.4 mmol) in acetone (100 mL) was added dippp (3.15 g; 11.4 mmol) dropwise. With each drop of phosphine a yellow precipitate formed and the deep amber color of the solution discharged completely to give a clear supernatant. After 30 min of stirring the reaction mixture was exposed to the air and the fine yellow precipitate was collected upon a frit, washed with copious acetone (100 mL), and air-dried (4.34 g; 84% yield). Anal. Calcd for $C_{15}H_{34}Cl_2P_2Pd$: C, 39.71; H, 7.55; Cl, 15.63. Found: C, 40.00; H, 7.65; Cl, 15.63. $^{31}P\{^1H\}$ and ^1H NMR assignments are reported elsewhere.[36]

Pd(dippp)I$_2$. To a slurry of Pd(dippp)Cl_2 (1.70 g; 3.75 mmol) in acetone (50 mL) was added NaI (1.50 g; 10.0 mmol). The color of the slurry deepened to ochre and stirring was continued for 2 h. Workup was as for Pd(dippp)Cl_2 giving Pd(dippp)I_2 as a fine ochre powder (2.12 g; 89% yield). Anal. Calcd for $C_{15}H_{34}I_2P_2Pd$: C, 28.30; H, 5.38; I, 39.87. Found: C, 27.98; H, 5.12; I, 40.05. ^1H NMR ($CDCl_3$): δ 2.90 (d hept, 4H, C*H*Me$_2$, J_{P-H} = 12.0 Hz, J_{H-Me} = 7.2 Hz), 2.25 (m, 2H, PCH_2CH_2-CH_2P), 1.61 (m, 4H, PCH_2CH_2P), 1.41 (dd, 12H, CH*Me*, J_{P-Me} = 19.2 Hz, J_{Me-H} = 7.2 Hz), 1.24 (dd, 12H, CH*Me'*, $J_{P-Me'}$ = 13.8 Hz, J_{Me-H} = 7.2 Hz). $^{31}P\{^1H\}$ NMR ($CDCl_3$): δ 30.7. Pd(dippp)I_2 may also be prepared directly without isolation of Pd(dippp)Cl_2 (76% yield).

[(dippp)Pd]$_2$(μ-H)$_2$ (2). Pd(dippp)I_2 (1.15 g; 1.80 mmol) was slurried in toluene (100 mL) and cooled to –60 °C in a dry-ice/acetone bath. A solution of $KBEt_3H$ (0.499 g; 3.81 mmol) in toluene (10 mL) was added dropwise with stirring and the temperature was raised to –40 °C. A slight effervescence was noted and the red color of the dimer developed as the Pd(dippp)I_2 reacted. The temperature was maintained at –40 °C for 2 h after which time gas evolution had ceased and the solution was deep red in color. The temperature was further raised to –20 °C for 30 min after which the reaction mixture was passed through a frit lined with Celite. The solvent was removed *in vacuo* and the residue dissolved in pentane (9 mL). The filtered solution was cooled to –30 °C and deep-red crystals appeared after 24 h (0.300 g, 44% yield). $^1H\{^{31}P\}$ NMR (C_6D_6): δ 1.93 (sept, 8H, C*H*Me$_2$, J_{H-Me} = 8.4 Hz), 1.90 (quin, 4H, PCH_2CH_2-CH_2P, $J_{H-H'}$ = 4.5 Hz), 1.32 (t, 8H, $PCH_2CH_2CH_2P$, $J_{H-H'}$ = 4.5 Hz), 1.30 and 1.10 (d, 48H, CH*Me*$_2$, J_{Me-H} = 8.4 Hz), –2.50 (s, 2H, μ-H). ^1H NMR (C_6D_6): δ –2.52 (quin, μ-H, J_{P-H} = 34.9 Hz), other resonances appeared as multiplets, T_1(μ-H) = 0.62 s. $^{31}P\{^1H\}$ NMR (C_6D_6): δ 27.0. Anal. Calcd for $C_{30}H_{70}P_4Pd_2$: C, 46.94; H, 9.19. Found: C, 47.22; H, 9.25.

[(dippp)Pd]$_2$(μ-D)$_2$ (2-d$_2$). The deuterium analogue was prepared by a procedure identical to that for **2** using $KBEt_3D$ (0.518 g; 3.72 mmol) and Pd(dippp)I_2 (1.16 g; 1.82 mmol). Recrystallization from pentane (10 mL) gave deep-red crystals (0.356 g, 51% yield). ^1H NMR (C_6D_6) δ 1.93 (m, 12H, $PCH_2CH_2CH_2P$, C*H*Me$_2$), 1.30 (m, 8H, PCH_2-CH_2CH_2P), 1.30 and 1.10 (m, 48H, CH*Me*$_2$), –2.55 (quin of t, residual μ-(H-D), J_{P-H} = 35.0 Hz, J_{H-D} = 2.4 Hz). ^2D NMR (C_7H_8): δ –2.52 (quin, μ-D, J_{P-D} = 5.5 Hz). ^{31}P NMR (C_6D_6) δ 27.0 (t, J_{P-D} = 5.5 Hz). Anal. Calcd for $C_{30}H_{70}P_4Pd_2$: C, 46.94; H, 9.19. Found: C, 46.75; H, 9.10.

[(dippp)Pd]$_2$(μ-H)$_2$·LiBEt$_4$ (1). To a slurry of Pd(dippp)Cl_2 (0.398 g; 0.877 mmol) in THF (60 mL) at –60 °C was added a mixture of $LiBEt_2H_2$ and $LiBEt_4$ in THF (1.80 mL; 1.80 mmol Li^+). The temperature was raised to –40 °C and the red color of the product developed as the Pd(dippp)Cl_2 reacted. A faint effervescence was also noted. The mixture was stirred for 2 h at the end of which time a deep red solution was observed and gas evolution had ceased. The temperature was further raised to –20 °C and stirring was continued for 1 h, after which the THF was removed under vacuum. The deep-red residue was extracted with toluene (30 mL) and the solution was passed through a frit lined with Celite to remove the precipitated LiCl. The toluene was removed by suction and the residue was dissolved in an extra volume of toluene (5 mL). This deep-red solution was layered with hexanes (10 mL) and yielded maroon crystals after 6 h at –40 °C (0.300 g; 68% yield). $^1H\{^{31}P\}$ NMR (C_6D_6): δ 1.85 (sept, 8H, C*H*Me$_2$, J_{H-Me} = 8.4 Hz), 1.78 (quin, 4H, $PCH_2CH_2CH_2P$, $J_{H-H'}$ = 4.4 Hz), 1.34 (br t, 12H, BCH_2CH_3, $J_{H-H'}$ = 7.5 Hz), 1.24 (t, 8H, $PCH_2CH_2CH_2P$, $J_{H-H'}$ = 4.4 Hz), 1.19 and 1.07 (d, 48H, CH*Me*$_2$, J_{Me-H} = 8.4 Hz), 0.42 (br q, 8H, BCH_2CH_3, $J_{H-H'}$ = 7.5 Hz), –3.63 (br s, 2H, μ-H). ^1H NMR (C_6D_6): δ –3.66 (br quin, μ-H, J_{P-H} = 35 Hz), other resonances appeared as multiplets, T_1(μ-H) = 0.49 s. $^{31}P\{^1H\}$ NMR (C_6D_6): δ 22.4. Anal. Calcd for $C_{38}H_{90}BLiP_4Pd_2$: C, 50.62; H, 10.06. Found: C, 50.57; H, 10.06.

Alternatively $LiBEt_4$ may be added to a solution of $[(dippp)Pd]_2(\mu\text{-}H)_2$ in toluene as for **3**. Recrystallization from toluene/pentane gives the product in yields over 90%.

[(dippp)Pd]$_2$(μ-H)$_2$·NaBEt$_4$ (3). **2** (0.100 g; 0.130 mmol) and $NaBEt_4$ (0.020 g; 0.133 mmol) were treated as for the preparation of **4**. Upon adding the $NaBEt_4$ to the solution of **2** the color darkened to a bottle-green. Removal of the solvent gave a blue, crystalline residue. The residue was taken up in toluene (1.2 mL) and the green solution was layered with pentane (5.0 mL). Blue crystals appeared after 6 h (0.050 g; 41% yield). ^1H NMR (C_6D_6): δ 1.74 (m, 12H, $PCH_2CH_2CH_2P$, C*H*Me$_2$), 1.39 (t, 12H, BCH_2CH_3, $J_{H-H'}$ = 7.0 Hz), 1.12 (m, 8H, PCH_2-CH_2CH_2P), 1.10 and 0.99 (m, 48H, CH*Me*$_2$), 0.19 (q, 8H, BCH_2CH_3, $J_{H'-H}$ = 7.0 Hz), –3.43 (quin, 2H, μ-H, J_{P-H} = 35.4 Hz), T_1(μ-H) = 0.18 s. ^{31}P NMR (C_6D_6): δ 25.4. Anal. Calcd for $C_{38}H_{90}BNaP_4Pd_2$: C, 49.74; H, 9.89. Found: C, 50.00; H, 10.07.

[(dippp)Pd]$_2$(μ-H)$_2$·LiAlEt$_4$ (4). **2** (0.100 g; 0.130 mmol) and $LiAlEt_4$ (0.020 g; 0.133 mmol) were dissolved in toluene (10 mL) and stirred for 1 h. The red color of the solution becomes slightly less intense during this time. The solvent was removed by suction and recrystallization from pentane/toluene (3:1; 10 mL) gave purple crystals after 48 h (0.109 g; 89% yield). ^1H NMR (C_6D_6): δ 1.80 (m, 8H, C*H*Me$_2$), 1.75 (m, 4H, $PCH_2CH_2CH_2P$), 1.60 (t, 12H, $AlCH_2CH_3$, $J_{H'-H}$ = 8.1 Hz), 1.16 (m, 8H, $PCH_2CH_2CH_2P$), 1.20 and 1.07 (m, 48H, CH*Me*$_2$), 0.05 (q, 8H, $AlCH_2CH_3$, $J_{H'-H}$ = 8.1 Hz), –3.87 (quin, 2H, μ-H, J_{P-H} = 35.0 Hz).

(15) Version 1.00 was obtained from Drs. G. Hägele and R. Fuhler of the Heinrich-Heine University, Düsseldorf, Germany; it will later be released as part of the WIN-NMR software package for the IBM PC.

(16) Tani, K.; Tanigawa, E.; Yatsuno, Y.; Otsuka, S. *J. Organomet. Chem.* **1985**, *279*, 87–95.

(17) Bryce-Smith, D.; Turner, E. E. *J. Chem. Soc.* **1953**, 861–867.

(18) Baker, E. B.; Sisler, H. H. *J. Chem. Soc.* **1953**, 5193–5195.

(19) Klusener, P. A. A.; Brandsma, L.; Verkruijsse, H. D.; Schleyer, P. v. R.; Friedl, T.; Pi, R. *Angew. Chem., Int. Ed. Engl.* **1986**, *25*, 465.

(20) Doyle, J. R.; Slade, P. E.; Jonassen, H. B. *Inorg. Synth.* **1960**, *6*, 216–219.

Table 1. Crystallographic Data[a]

compd	[(dippp)Pd]$_2$(μ-H)$_2$·LiBEt$_4$·0.5(C_6H_{14}) (**1**)	[(dippp)Pd]$_2$(μ-H)$_2$ (**2**)	[(dippp)Pd]$_2$(μ-H)$_2$·NaBEt$_4$ (**3**)
formula	$C_{41}H_{97}BLiP_4Pd_2$	$C_{30}H_{70}P_4Pd_2$	$C_{38}H_{90}BNaP_4Pd_2$
fw	944.66	767.58	917.62
habit	prism	prism	hexagonal plate
cryst size, mm	0.20 × 0.30 × 0.35	0.15 × 0.30 × 0.40	0.20 × 0.45 × 0.45
cryst system	monoclinic	monoclinic	monoclinic
space group	$P2_1/n$	$P2_1/n$	$P2_1/c$
a, Å	11.537(2)	13.128(1)	20.099(2)
b, Å	19.114(2)	14.362(4)	11.457(5)
c, Å	24.020(1)	20.353(1)	21.600(3)
b°	98.674(9)	99.593(6)	92.87(1)
V, Å^3	5236(1)	3784(1)	4968(2)
Z	4	4	4
T, °C	21	21	21
D_c, g/cm^3	1.198	1.347	1.227
F(000)	2012	1608	1944
m(Mo Kα), cm^{-1}	8.33	11.22	8.72
transmission factors	0.92–1.00	0.83–1.00	0.82–1.00
scan type	ω–2θ	ω–2θ	ω–2θ
scan range, deg in ω	1.00 + 0.35 tan θ	1.21 + 0.35 tan θ	1.10 + 0.35 tan θ
scan speed, deg/min	16	16	32
data collected	$+h,+k,\pm l$	$+h,+k,\pm l$	$+h,+k,\pm l$
$2\theta_{max}$, deg	55	55	55
cryst decay	negligible	4.5%	5.3%
total no. of reflcns	12959	9441	12336
unique reflcns	12356	9056	12005
R_{merge}	0.046	0.067	0.033
no. with $I \geq 3s(I)$	5954	4560	5018
no. of variables	451	329	425
R	0.033	0.052	0.033
R_w	0.029	0.054	0.028
gof	1.62	3.18	1.51
max D/s (final cycle)	0.05	0.02	0.04
residual density, e/Å^3	–0.34, 0.65 (both near Pd)	–1.0, 1.4 (near Pd)	–0.32, 0.27

[a] Temperature 294 K, Rigaku AFC6S diffractometer, Mo Kα radiation, l = 0.71069 Å, graphite monochromator, takeoff angle 6.0°, aperture 6.0 × 6.0 mm at a distance of 285 mm from the crystal, stationary background counts at each end of the scan (scan/background time ratio 2:1), $s^2(F^2) = [S^2(C + 4B)]/Lp^2$ (S = scan speed, C = scan count, B = normalized background count), function minimized $Sw(|F_o| - |F_c|)^2$ where $w = 4F_o^2/s^2(F_o^2)$, $R = S||F_o| - |F_c||/S|F_o|$, $R_w = (Sw(|F_o| - |F_c|)^2/Sw|F_o|^2)^{1/2}$, and gof = $[Sw(|F_o| - |F_c|)^2/(m - n)]^{1/2}$. Values given for R, R_w, and gof are based on those reflections with $I \geq 3s(I)$.

$^{31}P\{^1H\}$ NMR (C_6D_6): δ 23.3. Anal. Calcd for $C_{38}H_{90}AlLiP_4Pd_2$: C, 49.73; H, 9.88. Found: C, 49.48; H, 9.85.

Pd(dippp)(η^2-H_2C=CH_2). To a solution of **2** (0.081 g; 0.106 mmol) in toluene (10 mL), subjected to several freeze–pump–thaw cycles was added ethylene (0.500 mmol) from a constant volume bomb. The initial red color of the solution rapidly discharged to give a colorless solution. The solvent was stripped off, the residue was dissolved in a minimum of pentane (2.5 mL), and the clear solution was cooled to –30 °C. Colorless crystals appeared after 48 h (0.070 g; 80% yield). ^1H NMR (C_6D_6): δ 2.86 (d, 4H, H_2C=CH_2, J_{P-H} = 1.5 Hz), 1.69 (sept, 4H, C*H*Me$_2$, J_{H-Me} = 7.0 Hz), 1.68 (m, 2H, PCH$_2$C*H*$_2$CH$_2$P), 1.25 (m, 4H, PC*H*$_2$-CH$_2$C*H*$_2$P), 1.08 and 0.96 (dd, 24H, CH*Me*$_2$, J_{P-H} = 15.0 Hz, J_{Me-H} = 7.0 Hz). ^{31}P NMR (C_6D_6): δ 29.5. Anal. Calcd for $C_{17}H_{38}P_2Pd$: C, 49.70; H, 9.32. Found: C, 49.90; H, 9.41.

Pd(dippp)(PPh$_3$). To a solution of **2** (0.090 g; 0.117 mmol) in toluene (15 mL) was added PPh_3 (0.061 g; 0.233 mmol). The red color discharged rapidly and a vigorous evolution of gas was observed. The solvent was stripped off and the yellow residue taken up in Et_2O (15 mL). A yellow, microcrystalline powder deposited on standing (0.132 g; 87% yield). ^1H NMR (C_6D_6): δ 7.88 (m, 6H, *o*-Ph), 7.15 (m, 9H, *m*-, *p*-Ph), 1.75 (m, 6H, PCH$_2$C*H*$_2$CH$_2$P, C*H*Me$_2$), 1.23 (m, 4H, PC*H*$_2$CH$_2$C*H*$_2$P), 1.08 and 0.96 (dd, 24H, CH*Me*$_2$, J_{P-H} = 9.6 Hz, $J_{H-H'}$ = 3.0 Hz). ^{31}P NMR (C_6D_6): δ 33.8 (t, 1P, $J_{P-P'}$ = 88.5 Hz), 23.7 (d, 2P, $J_{P-P'}$ = 88.5 Hz). Anal. Calcd for $C_{33}H_{49}P_3Pd$: C, 61.33; H, 7.66. Found: C, 61.52; H, 8.00.

Pd(dippp)(DMAD). To a solution of **2** (0.075 g; 0.098 mmol) in toluene (10 mL) was added DMAD in toluene (0.029 g; 0.200 mmol). The initial red color of the solution slowly discharged to give a colorless solution within 1 h. The solvent was stripped off, and the residue was dissolved in minimum pentane (5 mL). The colorless solution was cooled to –40 °C and colorless crystals appeared after 48 h (0.087 g; 85% yield). ^1H NMR (C_6D_6): δ 3.54 (s, 6H, CO_2CH_3), 1.82 (sept, 4H, C*H*Me$_2$, J_{H-Me} = 7.0 Hz), 1.51 (m, 2H, PCH$_2$C*H*$_2$CH$_2$P), 1.22 (m, 4H, PC*H*$_2$-CH$_2$C*H*$_2$P), 1.11 and 0.87 (dd, 24H, CH*Me*$_2$, J_{P-H} = 16.0 Hz, J_{Me-H} = 7.0 Hz). ^{31}P NMR (C_6D_6): δ 34.5. Anal. Calcd for $C_{21}H_{40}P_2O_4Pd$: C, 48.05; H, 7.68. Found: C, 48.27; H, 7.90.

X-ray Crystallographic Analyses of [(dippp)Pd]$_2$(μ-H)$_2$·LiBEt$_4$·0.5-(C_6H_{14}) (1), [(dippp)Pd]$_2$(μ-H)$_2$ (2), and [(dippp)Pd]$_2$(μ-H)$_2$·NaBEt$_4$ (3). Crystallographic data appear in Table 1. The final unit-cell parameters were obtained by least squares on the setting angles for 25 reflections with 2θ = 20.5–28.4°, 30.0–39.4°, and 19.2–34.9° respectively for **1**–**3**. The intensities of three standard reflections, measured every 200 reflections throughout the data collections, remained constant for **1** and decreased linearly by 4.5% for **2** and by 5.3% for **3**. The data were processed[21] and corrected for Lorentz and polarization effects, decay (for **2** and **3**), and absorption (empirical, based on azimuthal scans for three reflections).

The three structures were solved by conventional heavy atom methods, the coordinates of the Pd and P atoms being determined from the Patterson functions and those of the remaining non-hydrogen atoms from subsequent difference Fourier syntheses. Disorder of one of the chelate ring carbon atoms in **3** (C(2)) was modeled by split-atom refinement. The site occupancy of the major component was refined with the constraint that the occupancy factors for the two sites sum to 1.00. The carbon atoms of the ligand containing P(3) and P(4) in **3** display a generally high degree of thermal motion that may be associated with some additional minor disordering. No attempt to model this possible disorder was made. The non-hydrogen atoms of all three structures were refined with anisotropic thermal parameters. The metal hydride atoms were refined with isotropic thermal parameters for **1**, were placed in difference map positions but not refined for **3**, and were refined with fixed thermal parameters near the end of the refinement but kept fixed during the final cycle due to a parameter oscillation problem for **2**. All other hydrogen atoms were fixed in idealized positions (staggered methyl groups, C–H = 0.99 Å for **1** and 0.98 Å for **2** and **3**, $B_H = 1.2 B_{bonded\ atom}$). A correction for secondary extinction was applied for **1**, the final value of the extinction coefficient (Zaccharisen type) being 8.5 (3) × 10^{-8}. The results for **1** presented here differ slightly from those reported earlier.[11] More accurate

(21) TEXSAN/TEXRAY: Crystal structure analysis package (VMS Version 5.1); Molecular Structure Corporation: The Woodlands, TX, 1985, 1991 (for **2** and **3**). *teXsan*: Crystal structure analysis package (UNIX Version 1.6); Molecular Structure Corporation: The Woodlands, TX, 1985, 1992 (for **2**).

Table 2. Selected Intramolecular Distances (Å) Observed in $[(dippp)Pd]_2(\mu\text{-}H)_2\cdot LiBEt_4$ (**1**), $[(dippp)Pd]_2(\mu\text{-}H)_2$ (**2**), and $[(dippp)Pd]_2(\mu\text{-}H)_2\cdot NaBEt_4$ (**3**)

	$[(dippp)Pd]_2(\mu\text{-}H)_2\cdot LiBEt_4$ (**1**)		
Pd(1)–Pd(2)	2.8248(5)	Pd(1)–H(1)	1.68(3)
Pd(1)–H(2)	1.70(3)	Pd(1)–P(1)	2.344(1)
Pd(1)–P(2)	2.337(1)	Pd(1)–Li	2.733(8)
Pd(2)–H(1)	1.79(4)	Pd(2)–H(2)	1.76(3)
Pd(2)–P(3)	2.336(1)	Pd(2)–P(4)	2.336(1)
Pd(2)–Li	2.635(8)	Li–B	2.275(9)
Li–H(1)	2.54(4)	Li–H(2)	2.25(3)
Li–C(31)	2.371(10)	Li–C(33)	2.339(9)
Li–C(35)	2.316(10)		
	$[(dippp)Pd]_2(\mu\text{-}H)_2$ (**2**)		
Pd(1)–Pd(2)	2.8245(8)	Pd(1)–H(1)	1.67(5)
Pd(1)–H(2)	2.13(4)	Pd(1)–P(1)	2.304(2)
Pd(1)–P(2)	2.299(2)	Pd(2)–H(1)	2.11(5)
Pd(2)–H(2)	1.73(4)	Pd(2)–P(3)	2.306(2)
Pd(2)–P(4)	2.300(4)		
	$[(dippp)Pd]_2(\mu\text{-}H)_2\cdot NaBEt_4$ (**3**)		
Pd(1)–Pd(2)	2.8169(6)	Pd(1)–H(1)	1.82(5)
Pd(1)–H(2)	1.79(4)	Pd(1)–P(1)	2.326(1)
Pd(1)–P(2)	2.325(1)	Pd(1)–Na	2.874(2)
Pd(2)–H(1)	1.74(5)	Pd(2)–H(2)	1.77(4)
Pd(2)–P(3)	2.324(3)	Pd(2)–P(4)	2.320(2)
Pd(2)–Na	2.897(2)	Na–B	3.329(2)
Na–H(1)	2.60(5)	Na–H(2)	2.56(5)
Na–C(31)	2.67(2)	Na–C(33)	2.78(2)

unit cell parameters, different weights, and the extinction correction have been employed. The crystal of **2** used for data collection was either twinned or fused to a fairly small satellite, resulting in relatively high residuals. Approximately 40 reflections with $|F_o| \gg |F_c|$, presumably resulting from overlapping reflections from the twin (or satellite) components, were omitted in the final stages of the refinement. Table 2 contains selected bond lengths while Table 3 reports selected bond angles for the complexes **1**, **2**, and **3**. Neutral atom scattering factors and anomalous dispersion corrections for all atoms were taken from the *International Tables for X-Ray Crystallography*.[22] Final atomic coordinates and equivalent isotropic thermal parameters, complete tables of bond lengths and angles, hydrogen atom parameters, anisotropic thermal parameters, torsion angles, intermolecular contacts, least-squares planes, and measured and calculated structure factor amplitudes are included as supplementary material.

Results and Discussion

Our entry into this area came about during attempts to prepare a binuclear palladium complex that contained bridging hydrides. The initial intention was to complement work previously done in our laboratory on the corresponding binuclear rhodium complexes having chelating bidentate phosphine ancillary ligands and hydride bridges.[23-26] However, it was also clear from examination of the literature that no palladium complexes bearing bridging hydrides had previously been unequivocally characterized,[27-29] in spite of the fact that there were reports of nickel and platinum dimers of the general formula $[P_2M]_2(\mu\text{-}H)_2$ (P_2 = bidentate phosphine).[30-32]

The addition of a THF solution of $LiBEt_3H$ (Aldrich Super Hydride) to a slurry of $Pd(dippp)Cl_2$ in THF at low temperatureled to the formation of a deep red solution from which maroon crystals having the formula $[(dippp)Pd]_2(\mu\text{-}H)_2\cdot LiBEt_4$ (**1**) could be isolated in 68% yield (eq 1). The ^1H NMR spectrum of **1**

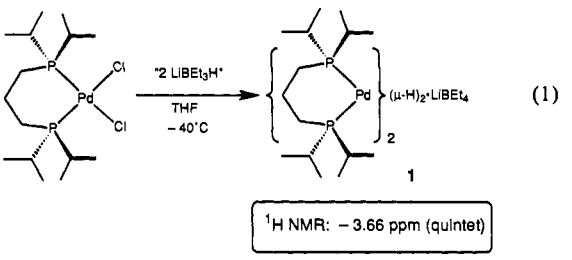

(1)

exhibited a broad quintet at −3.66 ppm ($^2J_{P-H}$ = 35 Hz), due to coupling to four equivalent phosphorus-31 nuclei, which clearly indicates the presence of bridging hydrides; furthermore, resonances due to a $LiBEt_4$ residue were observed at 1.30 and 0.42 ppm for the methyl and methylene resonances, respectively (cf. 1.29 and 0.21 ppm for crystalline $LiBEt_4$ in C_7D_8). The question of the origin of $LiBEt_4$ from a proprietary solution that was nominally $LiBEt_3H$ was easily resolved by ^{11}B NMR spectroscopy; the spectrum of our particular bottle displayed two resonances: a singlet at −17.5 ppm, overlayed by a triplet at −17.8 (J_{B-H} = 67.4 Hz), attributed to $LiBEt_4$ and $LiBEt_2H_2$, respectively. Other bottles examined contained only authentic $LiBEt_3H$.

The X-ray crystal structure of **1** is shown in Figure 1. The binuclear structure is clearly evident as are the bridging hydrides which were located and refined. The palladium–hydride bond lengths range from 1.68(3) to 1.79(4) Å (cf., Pd(1)–H(1) 1.68(3) Å; Pd(1)–H(2) 1.70(3) Å; Pd(2)–H(1) 1.79(4) Å; Pd(2)–H(2) 1.76(3) Å); the Pd–H–Pd angle is 109(2)°. However, the most interesting feature of this structure is the presence of a coordinated $LiBEt_4$ unit having the lithium cation sandwiched between the $Pd_2(\mu\text{-}H)_2$ core and the BEt_4 anion. The palladium–lithium distances are significantly different with the lithium being closer to Pd(2): Pd(1)–Li 2.733(8) Å and Pd(2)–Li 2.635(8) Å. Also noteworthy is the interaction of the lithium with the BEt_4 unit as the lithium binds to one C–H bond on each of three α-carbon ethyl substituents (Li–H = 1.69, 1.72 and 1.86 Å). The neutron diffraction study of $LiBMe_4$ shows similar Li–H–C interactions.[33]

The unsymmetrical solid-state structure is not maintained in solution as evidenced by NMR spectroscopy. A symmetrical structure in solution is required since the two ends of the binuclear unit are spectroscopically equivalent, that is, a singlet in the $^{31}P\{^1H\}$ NMR spectrum which indicates that all the phosphines are equivalent; in addition, the $LiBEt_4$ remains coordinated since the resonances due to the tetraethylborate unit are shifted in the ^1H NMR spectrum from those measured for pure $LiBEt_4$ in C_7D_8. Variable-temperature ^1H NMR studies show that, in solution, all four ethyl groups at boron are equivalent even at low temperatures, indicating that the BEt_4 unit is rather mobile. Moreover, from the variable-temperature NMR data, it is also evident that the top and the bottom of the binuclear palladium hydride are apparently equivalent, thus suggesting that the whole $LiBEt_4$ unit is labile. This feature will be discussed further below.

Clearly, any attempt to rationalize the nature of the bonding by the $LiBEt_4$ unit in the palladium–lithium adduct **1** could not be broached without the parent hydride dimer, $[(dippp)Pd]_2(\mu\text{-}H)_2$. Unfortunately, attempts to prepare this complex by hydride metathesis of $Pd(dippp)Cl_2$ with pure $LiBEt_3H$ were unsuccessful; however, treatment of the more soluble diiodide derivative Pd-

(22) *International Tables for X-Ray Crystallography*; Kynoch Press: Birmingham, U.K. (present distributor D. Reidel: Dordrecht, The Netherlands), 1974; Vol. IV, pp 99–102 and 149.
(23) Fryzuk, M. D.; Piers, W. E.; Rettig, S. J.; Jones, T.; Einstein, F. W. B.; Albright, T. S. *J. Am. Chem. Soc.* **1989**, *111*, 5709–5721.
(24) Fryzuk, M. D.; Piers, W. E.; Einstein, F. W. B.; Jones, T. *Can. J. Chem.* **1989**, *67*, 883–896.
(25) Fryzuk, M. D.; Piers, W. E. *Organometallics* **1990**, *9*, 986–998.
(26) Fryzuk, M. D.; McConville, D. H.; Rettig, S. J. *Organometallics* **1990**, *9*, 1359–1360.
(27) Zudin, V. N.; Chinakov, V. D.; Nekipelov, V. M.; Likholobov, V. A.; Yermakov, Y. U. *J. Organomet. Chem.* **1989**, *285*, 425.
(28) Young, S. J.; Kellenberger, B.; Reibenspies, J. H.; Himmel, S. E.; Manning, M.; Anderson, O. P.; Stille, J. K. *J. Am. Chem. Soc.* **1988**, *110*, 5744.
(29) Schunn, R. A. *Inorg. Chem.* **1976**, *15*, 208.
(30) Jonas, K.; Wilke, G. *Angew. Chem., Int. Ed. Engl.* **1970**, *9*, 312.
(31) Carmichael, D.; Hitchcock, P. B.; Nixon, J. F.; Pidcock, A. *J. Chem. Soc., Chem. Commun.* **1988**, 1554.
(32) Clark, H. C.; Hampden-Smith, M. *J. Am. Chem. Soc.* **1986**, *108*, 3829.
(33) Rhine, W. E.; Stucky, G. D.; Peterson, S. W. *J. Am. Chem. Soc.* **1975**, *97*, 6401.

$(dippp)I_2$ with 2 equiv of crystalline $KBEt_3H$ in toluene does give $[(dippp)Pd]_2(\mu\text{-}H)_2$ (**2**), as shown in eq 2. Particularly, diagnostic of **2** is the hydride resonance in the ^1H NMR spectrum at −2.52 ppm which appears as a binomial quintet (J_{P-H} = 34.9 Hz).

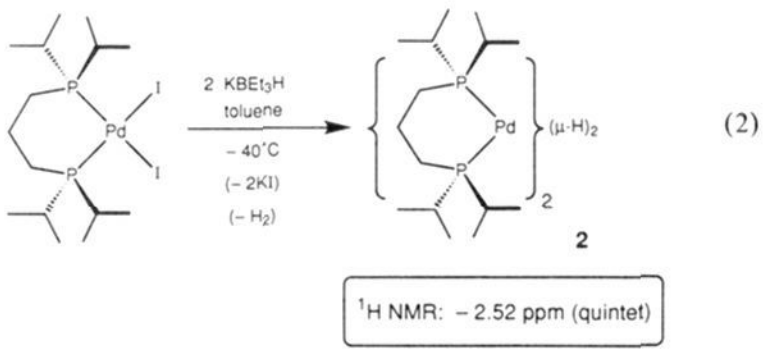

(2)

Typical formal oxidation states for palladium are +2 and 0.[34] However, both of the binuclear complexes, **1** and **2**, have formal oxidation states of +1, assuming that the hydrogens are bridging hydrides, $Pd_2(\mu\text{-}H)_2$, and not a bridging dihydrogen unit, $Pd_2(\mu\text{-}\eta^2\text{-}H_2)$.

From the X-ray structure of **1**, the presence of bridging hydrides is reasonable since the H–H separation is 2.00(5) Å, longer than the 1.6-Å distance normally ascribed as the cutoff for a η^2-H_2 ligand.[35] Evidence that the parent binuclear complex **2** is also best described as a Pd(I) dimer comes from the formation of $[(dippp)Pd]_2(\mu\text{-}D)_2$ by reaction of $KBEt_3D$ with the diiodide as before. The ^1H NMR spectrum of **2**-d_2 shows a small quintet of 1:1:1 triplets at −2.55 ppm due to residual protons coupled to deuterium and four equivalent phosphorus-31 nuclei indicative of $[(dippp)Pd]_2(\mu\text{-}D)(\mu\text{-}H)$ (**2**-d_1); the observed H–D coupling constant (J_{H-D}) of 2.4 Hz is much too small to be due to a η^2-H_2 moiety.[35]

The solution structure of bare palladium dimer **2** indicates that the phosphine donors are equivalent at all temperatures as are the hydrides; thus, any of the following geometries is appropriate for this molecule.

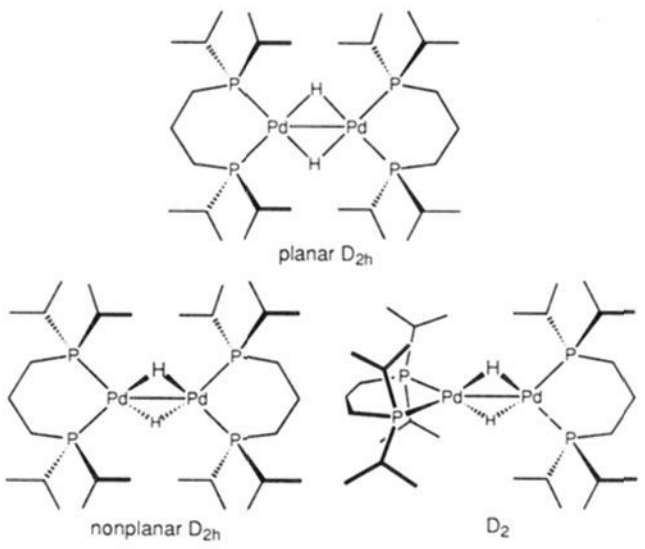

The X-ray crystal structure of this bare palladium hydride dimer **2** is shown in Figure 2. The Pd–Pd bond distance in **2** is 2.8245(8) Å, virtually identical to that found in the palladium–lithium adduct **1** (i.e. 2.8233(6) Å). What is striking, however, is the unsymmetrical nature of the hydride bridges between the two palladium atoms: the Pd(1)–H(1) distance is 1.67(3) Å while Pd(1)–H(2) is 2.13(4) Å; similarly, Pd(2)–H(2) is 1.73(3) Å and Pd(2)–H(1) is 2.11(3) Å. The shorter metal–hydride distances are similar to that found in the $LiBEt_4$ adduct **1** but longer than the 1.531(11) Å found in the recently reported[36] cation $\{[(dippp)Pd]_2(\mu\text{-}H)(\mu\text{-}CO)\}^+$.

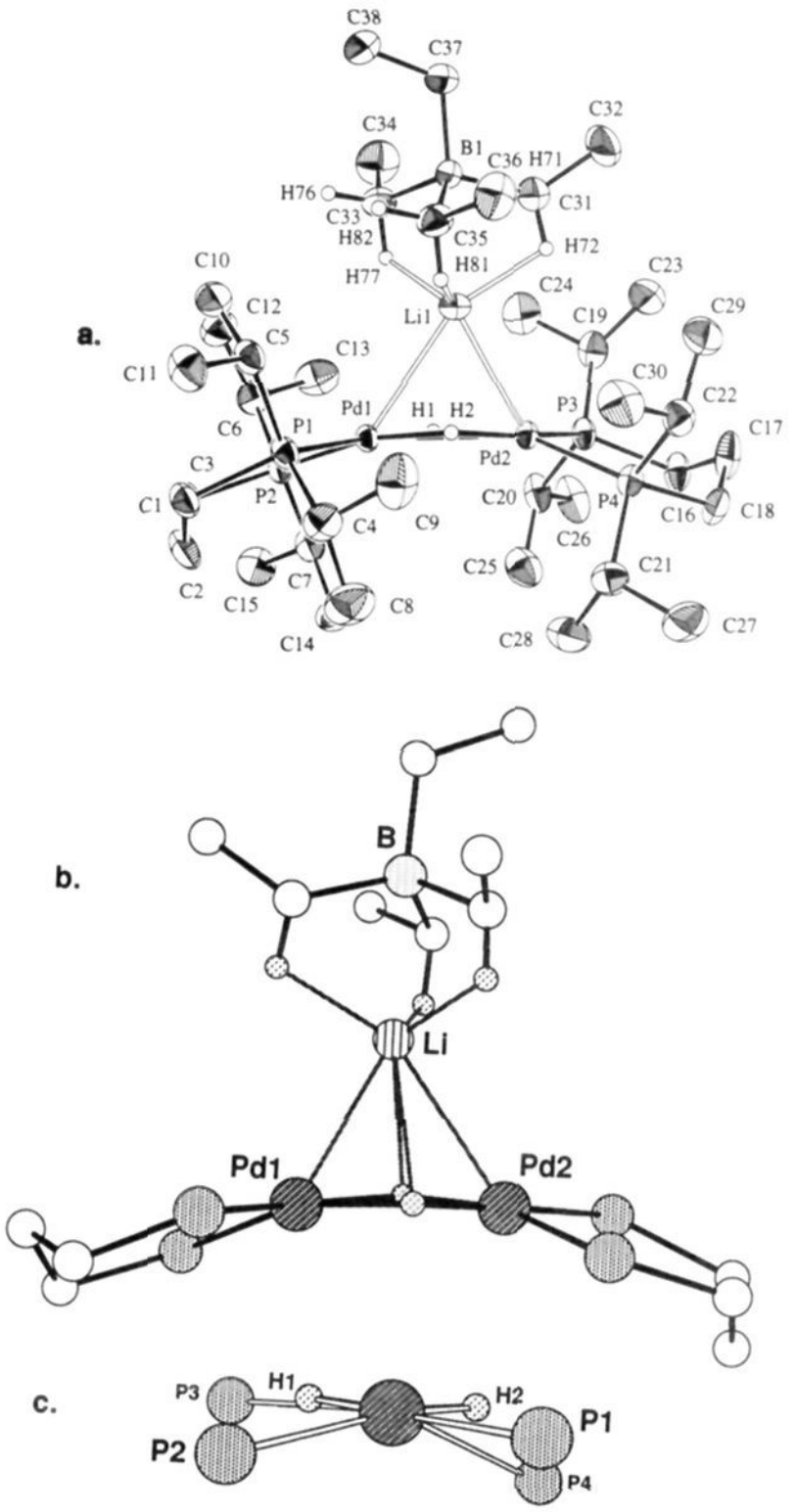

Figure 1. (a) Molecular structure and numbering scheme for $[(dippp)Pd]_2(\mu\text{-}H)_2\cdot LiBEt_4$ (**1**); (b) core view of **1** showing the interaction of the Li cation with the three α-C–H bonds in the ethyl groups, the bridging hydrides, and the palladium centres; and (c) a view looking down the Pd(1)–Pd(2) axis to show the nonplanar nature of the hydride and phosphorus core.

Table 3. Selected Intramolecular Angles (deg) Observed in $[(dippp)Pd]_2(\mu\text{-}H)_2\cdot LiBEt_4$ (**1**), $[(dippp)Pd]_2(\mu\text{-}H)_2$ (**2**), and $[(dippp)Pd]_2(\mu\text{-}H)_2\cdot NaBEt_4$ (**3**)

	$[(dippp)Pd]_2(\mu\text{-}H)_2\cdot LiBEt_4$ (**1**)		
H(1)–Pd(1)–H(2)	72(2)	H(1)–Pd(2)–H(2)	68.5(1.5)
P(1)–Pd(1)–P(2)	99.91(4)	P(3)–Pd(2)–P(4)	100.54(5)
Pd(1)–Li–Pd(2)	63.5(2)	Pd(1)–H(1)–Pd(2)	109(2)
Pd(1)–H(2)–Pd(2)	109(2)	H(1)–Li–H(2)	49(1)
	$[(dippp)Pd]_2(\mu\text{-}H)_2$ (**2**)		
H(1)–Pd(1)–H(2)	85.9(2)	H(1)–Pd(2)–H(2)	84.8(2)
P(1)–Pd(1)–P(2)	99.81(8)	P(3)–Pd(2)–P(4)	101.93(8)
Pd(1)–H(1)–Pd(2)	95.8(3)	Pd(1)–H(2)–Pd(2)	93.5(3)
	$[(dippp)Pd]_2(\mu\text{-}H)_2\cdot NaBEt_4$ (**3**)		
H(1)–Pd(1)–H(2)	73(2)	H(1)–Pd(2)–H(2)	76(2)
P(1)–Pd(1)–P(2)	100.49(5)	P(3)–Pd(2)–P(4)	100.95(6)
Pd(1)–Na–Pd(2)	58.43(4)	Pd(1)–H(1)–Pd(2)	104(2)
Pd(1)–H(2)–Pd(2)	105(3)	H(1)–Na–H(2)	49(3)

The solid-state structure is not completely planar as evidenced by the end-on view in Figure 2b. Looking down the Pd(1)–Pd(2)

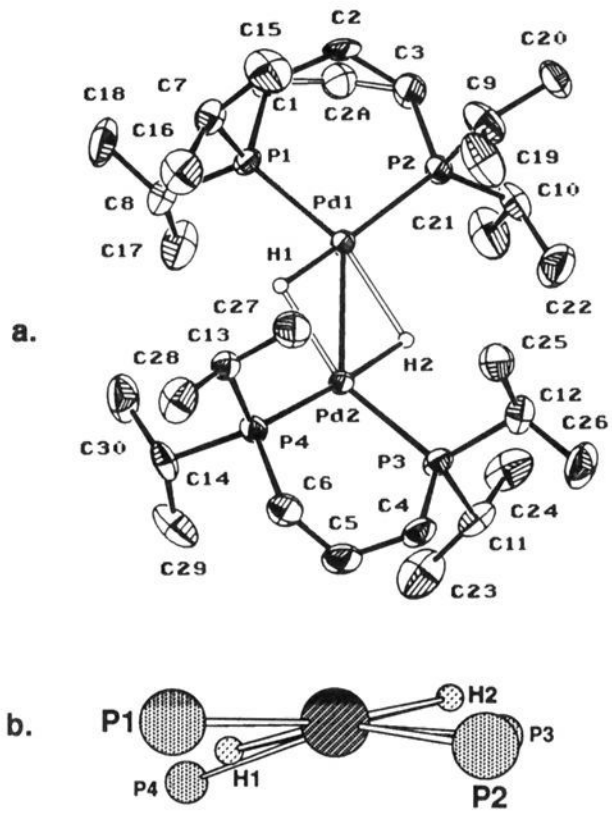

Figure 2. (a) Molecular structure and numbering scheme for [(dippp)-Pd]$_2$(μ-H)$_2$ (**2**); (b) a view looking down the Pd(1)–Pd(2) axis to show the nonplanar nature of the hydride and phosphorus core.

axis, the plane defined by the two palladium atoms and the two hydrides is canted by 19.5° to the P(1)–Pd(1)–P(2) plane and 15.1° to the P(3)–Pd(2)–P(4) plane. The analogous d^9 nickel dimer, [(dcypp)Ni]$_2$(μ-H)$_2$ (dcypp = 1,3-bis(dicyclohexylphosphino)propane), has a solid-state structure[37] more resembling a D_2 symmetric species with the two Ni(dicypp) ends of the molecule staggered by 63.3°. However, a molecular orbital calculation performed upon the model complex [$(H_3P)_2$Ni]$_2$(μ-H)$_2$ concluded that the energy minimum occurred for the completely planar D_{2h} structure, and thus the observed departure from planarity in [(dcypp)Ni]$_2$(μ-H)$_2$ was proposed to be due to steric repulsion between the cyclohexyl groups on alternate ligands.[37] For the structure of the lithium adduct **1**, this angle is 34.6°, while for the hydride dimer **2**, this angle is 24.0°. Presumably, because of the larger size of Pd as compared to Ni, steric repulsion between isopropyl groups across the ends of the binuclear unit is minimal and the structure of the parent palladium hydride dimer **2** is nearly planar.

In solution, the structure of the bare palladium dimer **2** is completely symmetrical as evidenced by equivalent phosphines and hydrides by NMR spectroscopy at all temperatures. For this reason, a symmetrical, planar D_{2h} geometry is assumed for all discussions of the solution structure of this dimer **2**.

Examination of the ^{1}H NMR spectrum of the original reaction mixture of Pd(dippp)Cl$_2$ and the THF solution of $LiBEt_2H_2$/$LiBEt_4$ that ultimately produces **1** revealed a quintet at –2.52 ppm which is identical to that observed for the parent palladium hydride dimer **2**. This is strong evidence that the bare hydride dimer **2** is the initial product and only upon workup with removal of the THF, which was undoubtedly coordinated to the $LiBEt_4$, does coordination of free $LiBEt_4$ to the palladium–hydride dimer occur.

The proposal that the bare hydride dimer **2** is an intermediate in the formation of the palladium–lithium adduct **1** can be confirmed by the preparation of adduct **1** from dimer **2** by addition of $LiBEt_4$ in an aromatic solvent. Isolated yields of **1** by this procedure are in excess of 90%. This appears to be a general

(34) Collman, J. P.; Hegedus, L. S.; Norton, J. R.; Finke, R. J. *Principles and Applications of Organotransition Metal Chemistry*; University Science Books: Mill Valley, CA, 1987; pp 412–415.
(35) Jessop, P. G.; Morris, R. H. *Coord. Chem. Rev.* **1992**, *121*, 155.
(36) Portnoy, M.; Frolow, F.; Milstein, D. *Organometallics* **1991**, *10*, 3960.
(37) Barnett, B. L.; Kruger, C.; Tsay, Y.-H.; Summerville, R. H.; Hoffmann, R. *Chem. Ber.* **1977**, *110*, 3900.

Scheme 1

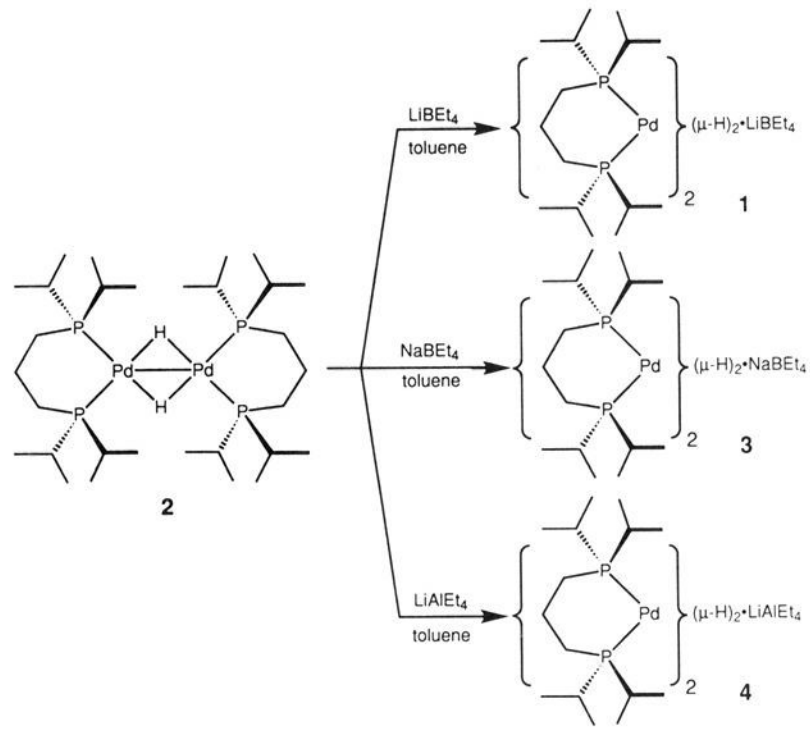

procedure since addition of the corresponding sodium salt, $NaBEt_4$, to the bare palladium dimer **2** generates the corresponding adduct [(dippp)Pd]$_2$(μ-H)$_2$•$NaBEt_4$ (**3**) while the addition of $LiAlEt_4$ also generates the related adduct [(dippp)-Pd]$_2$(μ-H)$_2$•$LiAlEt_4$ (**4**). All of these transformations are summarized in Scheme 1.

The solid-state X-ray structure of the $NaBEt_4$ adduct **3** is shown in Figure 3. As can be seen from the ORTEP diagram, it displays similar features to that of the $LiBEt_4$ adduct **1**. The binuclear structure is apparent as are the bridging hydrides; the Pd–Pd distance of 2.8169(6) Å is very slightly shorter than either of the comparable Pd–Pd bond distances in **1** or **2** and the Pd–H bond lengths of 1.80(3) Å are long but within the range of 1.67-(3)–2.13(4) Å observed for the bare dimer **2**.

The disposition of the tetraethylborate unit around the alkali metal constitutes the most important difference in the structures of adducts **1** and **3**. The lithium cation in **1** (Figure 1) is proximate to three of the α-carbons of the tetraethylborate unit, and a bridged interaction with one C–H bond of each of the three methylene units is inferred. It should be noted that the methylene hydrogens are in calculated positions based on the observed C–C angle of the ethyl group; nonetheless, only one C–H unit points at the Li cation. The Li–C separation (2.32–2.37 Å) is comparable to the corresponding distances in the structures of $LiBMe_4$ and $LiAlEt_4$ (2.36 and 2.37 Å, respectively).[33,38] The sodium nucleus in the solid-state structure of **3** (Figure 3) is contiguous to only two α-carbons, but now positioned to interact with four α-C–H bonds; again, the hydrogens are placed in calculated positions based on the observed C–C bond angle of the ethyl group. The difference in the interaction of Na^+ and Li^+ with the tetraethylborate unit may be attributed to some peculiarity of the solid state; however, it may also reflect that sodium ion is larger than lithium ion and thus prefers a higher coordination number. The average Na–C distance is 2.67 Å.

Other distances of note are the lithium–hydride bond lengths of 2.25(3) and 2.54(4) Å and the lithium–palladium separations of 2.733(8) and 2.635(8) Å, the differences again indicative of the unsymmetrical structure in the solid-state structure of **1**. The observed sodium–hydride distances are 2.56(5) and 2.60(4) Å and the sodium–palladium lengths are 2.90(5) and 2.87(3) Å.

Variable-temperature, ^{1}H NMR experiments on the $NaBEt_4$ adduct **3** show no inequivalence among the ethyl groups of the tetraethylborate groups, even at –90 °C, similar to that observed for the $LiBEt_4$ adduct **1**; this is consistent with the tetraethylborate

(38) Gerteis, R. L.; Dickerson, R. E.; Brown, T. L. *Inorg. Chem.* **1964**, *3*, 872.

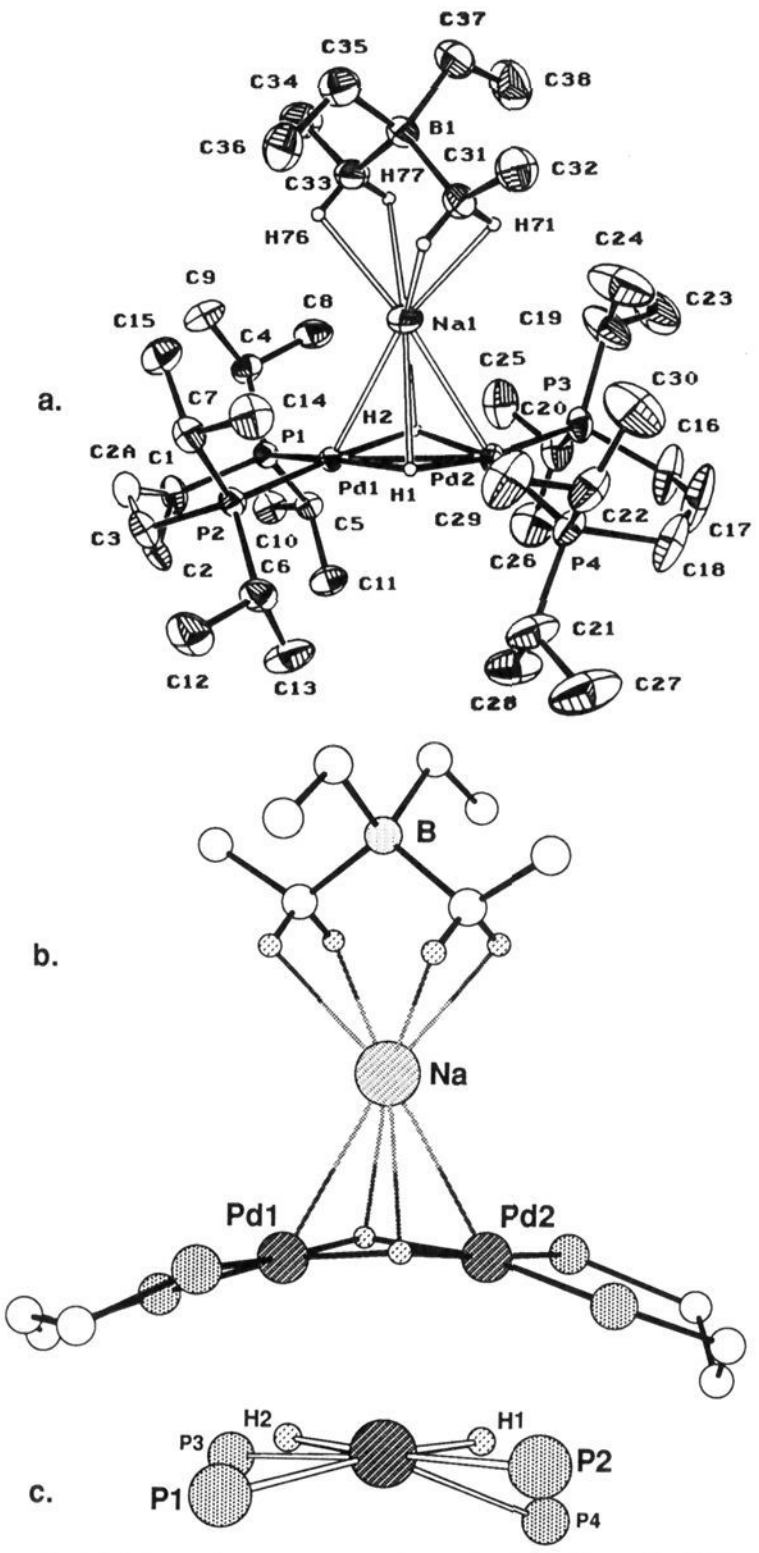

Figure 3. (a) Molecular structure and numbering scheme for [(dippp)-Pd]$_2$(μ-H)$_2$·NaBEt$_4$ (**3**); (b) core view of **3** showing the interaction of the Na cation with the four α-C–H bonds in the ethyl groups, the bridging hydrides, and the palladium centers; and (c) a view looking down the Pd(1)–Pd(2) axis to show the nonplanar nature of the hydride and phosphorus core.

anion undergoing a rapid tumbling motion in solution interchanging all the methylene protons. Also comparable to **1** is the fact that, in the sodium adduct **3**, the top and bottom of the binuclear hydride unit are equivalent by ^{1}H NMR spectroscopy even at low temperature which is a feature consistent with a labile NaBEt$_4$ unit.

As outlined in Scheme 1, upon addition of stoichiometric amounts of solid LiBEt$_4$ to a benzene or toluene solution of the parent hydride dimer **2**, the LiBEt$_4$ adduct **1** is produced as determined by ^{31}P{^{1}H} NMR spectroscopy. How strong, thermodynamically, is the interaction of the perethylborate and aluminate salts with the palladium hydride dimer **2**? Attempts to measure the equilibrium constant for adduct **1** in the presence of **2** by NMR spectroscopy have so far failed presumably because the adduct forms completely even at low concentrations of LiBEt$_4$. In addition, if a mixture of adduct **1** and the bare hydride dimer **2** are mixed together, exchange of the LiBEt$_4$ unit occurs as evidenced by broad resonances in the hydride region of the ^{1}H NMR spectrum (Figure 4); as the temperature is lowered, this particular exchange process becomes slow and the separate signals due to the hydride resonances of **1** and **2** are observed *in the exact ratio that they were originally mixed*. As the temperature is raised, the peaks coalesce to eventually generate a single resonance (at 100 °C) due to averaged intermolecular exchange. The kinetics of the exchange reaction have been estimated by variable-temperature ^{1}H NMR spectroscopy in C_7D_8, followed by simulation of the experimental spectra. A graph of the interpolated rate constant, k_{ex}, versus inverse temperature gave an exponential dependence over a temperature range of 243–373 K. The rate of exchange, R_{ex}, was found to vary as the concentration of adduct **1** and was insensitive to the concentration of the bare hydride dimer **2**. A simple first-order dissociative mechanism is proposed and the rate law is formulated as $R_{ex} = k_{ex}[\mathbf{1}]$. The Eyring activaton parameters may be extracted from a plot of $\ln(k_{ex}T^{-1})$ versus T^{-1}: $\Delta H^{\ddagger}_{ex} = 7.9 \pm 1.0$ kcal mol^{-1} and $\Delta S^{\ddagger}_{ex} = -13.6 \pm 4.0$ cal K^{-1} mol^{-1}.[39] The negative value of $\Delta S^{\ddagger}_{ex}$ is troublesome for what is suggested to be a dissociative mechanism; however, if solvent molecules participate in the activated complex by solvating free LiBEt$_4$, then this negative $\Delta S^{\ddagger}_{ex}$ can be rationalized. A more comprehensive kinetic analysis, embracing solvents other than C_7D_8, could not be performed due to the insolubility of **1** in aliphatic solvents, and its complete decomposition in chlorinated solvents. As expected, in the presence of donor solvents such as THF or Et$_2$O, adduct formation is disrupted and the bare palladium dimer **2** is produced as evidenced by ^{31}P{^{1}H} NMR spectroscopy.

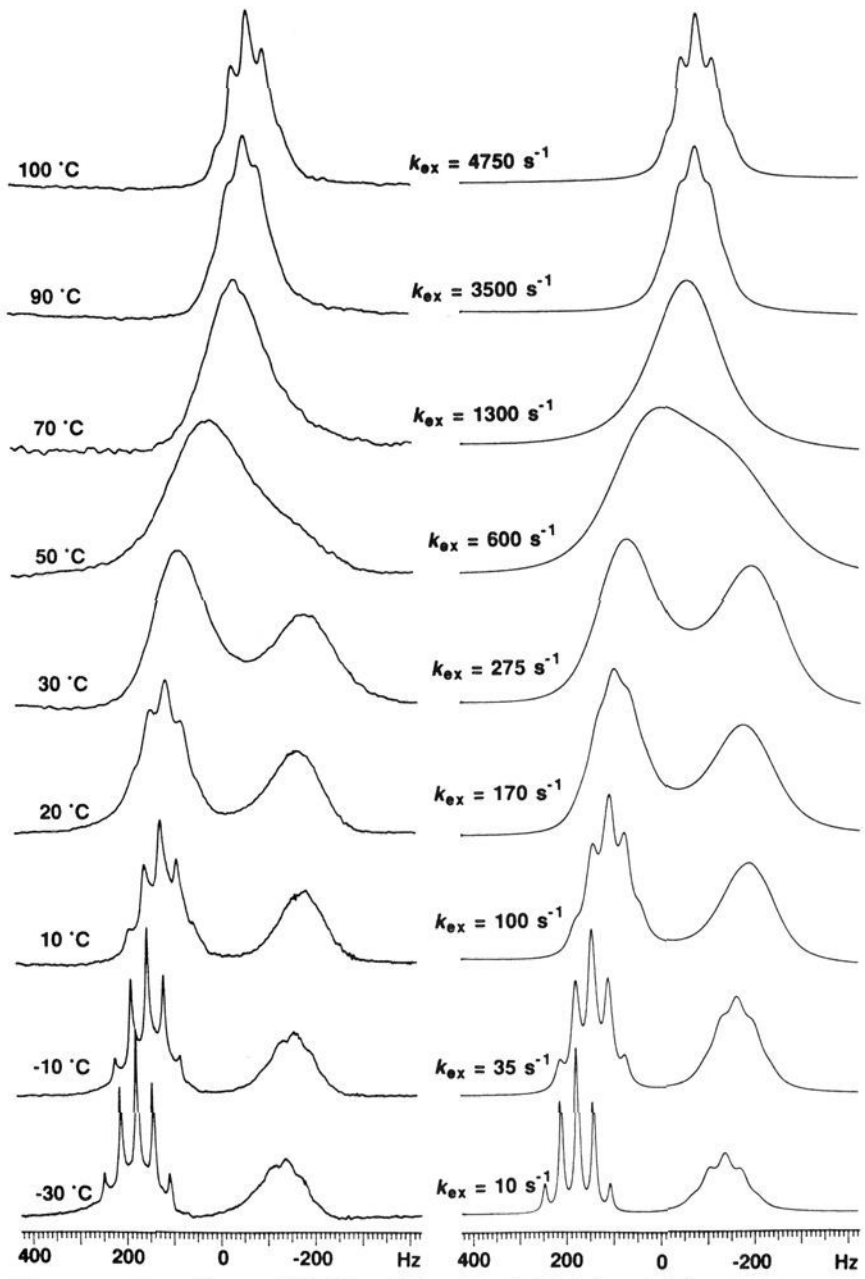

Figure 4. Experimental (left) and simulated (right) variable-temperature ^{1}H NMR spectra of an equimolar mixture of [(dippp)Pd]$_2$(μ-H)$_2$·LiBEt$_4$ (**1**) and [(dippp)Pd]$_2$(μ-H)$_2$ (**2**) in the hydride region (0 Hz = –3.0 ppm; [Pd] = 4.20×10^{-2} mol L^{-1}); the very sharp quintet at low temperatures is due to **2** while the broader resonance is due to LiBEt$_4$ adduct **1**.

These experiments provide further evidence that, thermodynamically, the adduct **1** is favored yet, kinetically, the LiBEt$_4$ is

(39) Espenson, J. H. *Chemical Kinetics and Reaction Mechanisms*; McGraw-Hill Book Company: New York, 1981; pp 50–55.

rather labile; this latter point corroborates the ^1H NMR spectral data concerning the equivalence of both the ethyl groups at boron and the isopropyl substituents at phosphorus at low temperatures mentioned earlier.

The addition of $LiBEt_4$ to the sodium adduct **3** results in virtually quantitative formation of the lithium adduct **1** (eq 4). Although 1 equiv of $LiBEt_4$ added to the sodium adduct **3** is enough to generate the lithium adduct **1** as the only detectable product, this is an equilibrium process since addition of ~5 equiv of $NaBEt_4$ to the lithium adduct **1** does result in the formation of a mixture of **1** and **3** in a 2:1 ratio; in other words, the reaction shown in eq 3 can be reversed to some extent by the addition of an excess of $NaBEt_4$.

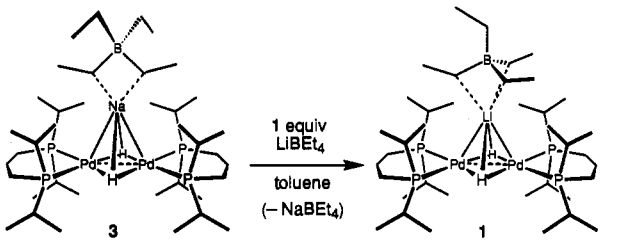

(3)

Interestingly, if $LiAlEt_4$ is added to the sodium tetraethyl*borate* adduct **3**, an equal mixture of the lithium adducts **1** and **4** is obtained indicating that there is little preference for the anion portion of the adduct (eq 4).

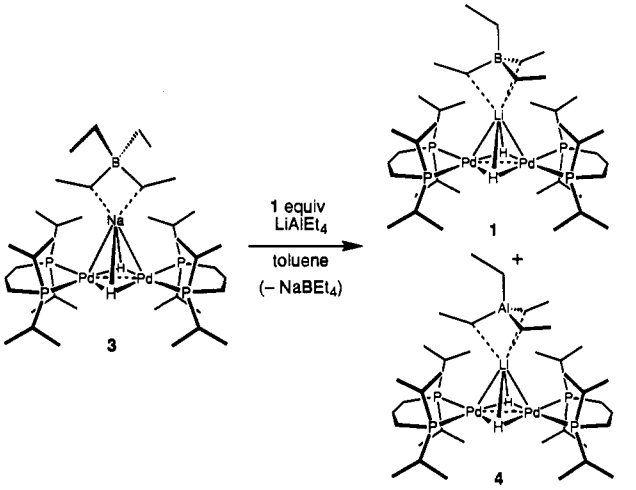

(4)

Bonding Considerations. With regard to the nature of the bonding in complexes **1**, **3**, and **4**, we have been unable to find another derivative with a similar type of interaction. Complexes that contain lithium are quite well known.[40-42] Examples range from ionic derivatives such as the tetrameric $\{[(\eta^5\text{-}C_5H_5)_2MoH]\text{-}Li\}_4$ to organolithium adducts of Ni(0) similar to **5** which are considered to be ion pairs.[43-45]

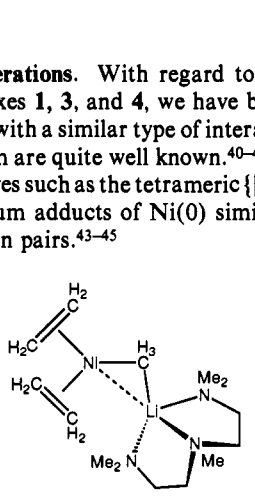

5

It should be stressed that the interaction of the lithium ion with the metal complex in **5** is fundamentally different than in the palladium–$LiBEt_4$ adduct **1** or the corresponding $NaBEt_4$ derivative **3** since, in **5**, the methyl anion is directly attached to the metal center, whereas in the latter molecules, the anionic BEt_4 moiety coordinates only to the Li^+ or Na^+ ions. If the interaction of the $LiBEt_4$ with the palladium hydride dimer is not ionic then it must be an ion–dipole type bond (i.e., the lithium ion is electrostatically attracted to electron density) since it is fairly well established that the bonding in organolithium derivatives is largely ionic.[40,46]

Scheme 2

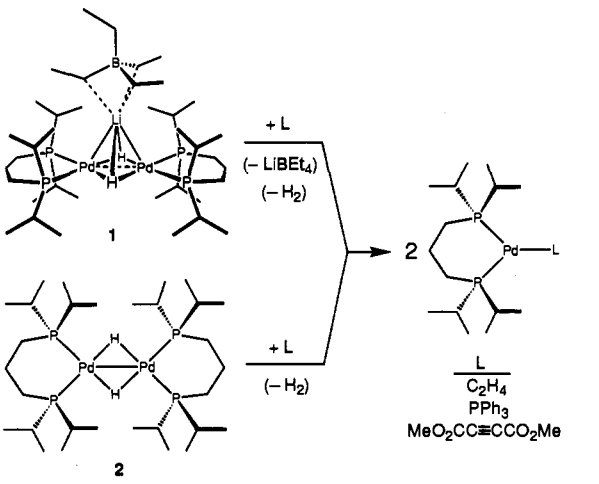

Reactivity Studies. Reactions of ethylene (or propylene) with the lithium adduct **1** result in the loss of H_2 (detected by ^1H NMR spectroscopy) and the release of the $LiBEt_4$ unit to generate the three-coordinate Pd(0) adduct $Pd(\eta^2\text{-}C_2H_4)$(dippp); a similar reaction ensues when PPh_3 is allowed to react with **1** since Pd-(PPh_3)(dippp) is obtained, and the reaction with dimethyl acetylenedicarboxylate, $MeO_2CC{\equiv}CCO_2Me$, also generates the corresponding Pd(0) adduct $Pd(\eta^2\text{-}MeO_2CC{\equiv}CCO_2Me)$(dippp). The same sequence of reactions carried out with the bare palladium dimer **2** produces the exact same palladium(0) adducts in virtually identical yields; all of this is summarized in Scheme 2. Thus, these formally palladium(I) hydride derivatives would appear to be sources of Pd(0) since H_2 elimination is observed rather than any insertion type chemistry. In the case of the Li adduct **1**, the presence of the Lewis acidic $LiBEt_4$ moiety does not apparently influence any of the simple reaction types shown here since it is liberated along with the H_2. There is precedent for the release of H_2 from formally Ni(I) hydride dimers upon addition of olefins as well as liberation of alkylaluminum fragments from adducts of Ni(0) derivatives.[13] In retrospect, it is difficult to imagine how the Lewis acidic portion of **1**, the $LiBEt_4$ unit, could have any influence on these types of reactions since the particular substrates used would be expected to be relatively innocuous to group 13 "ate" species. In addition, the similarity in the reaction outcomes shown in Scheme 2 is consistent with the lability of the $LiBEt_4$ unit in that it is the palladium hydride dimer portion of adduct **1** that is undergoing the H_2 displacement and ligand addition reactions.

Conclusions

The interaction of Lewis acids with transition-metal complexes is manifested in a number of significant reaction types. Shown

(40) Setzer, W. N.; Schleyer, P. v. R. *Adv. Organomet. Chem.* **1985**, *24*, 353.
(41) Darensbourg, M. Y.; Ash, C. E. *Adv. Organomet. Chem.* **1987**, *27*, 1.
(42) Jonas, K.; Krüger, C. *Angew. Chem., Int. Ed. Engl.* **1980**, *19*, 520.
(43) Wilke, G. *Angew. Chem., Int. Ed. Engl.* **1988**, *27*, 185.
(44) Poerschke, K. R.; Wilke, G. *J. Organomet. Chem.* **1988**, *358*, 519.
(45) Poerschke, K. R.; Wilke, G. *J. Organomet. Chem.* **1988**, *349*, 257–61.
(46) Schade, C.; Schleyer, P. v. R. *Adv. Organomet. Chem.* **1988**, *27*, 169.

below (E–H) are some illustrative examples[9,14,47,48] of how Lewis acids can influence the structure and reactivity of metal complexes.

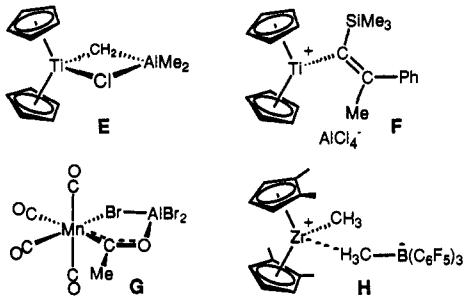

These examples illustrate that Lewis acids cannot only remove a ligand from the coordination sphere of a metal thereby generating a open site (e.g. **F** and **H**) but can also bind to particular ligands in the coordination sphere and stabilize reactive fragments (e.g. the Ti=CH_2 unit in Tebbe's reagent **E**) and promote migratory insertion (e.g. the manganese acyl derivative **G**).

In the work reported in this paper, we document a whole new kind of Lewis acid–Lewis base interaction that involves a neutral, binuclear metal complex having bridging hydride ligands and alkali metal salts of group 13 tetraalkyl "ate" derivatives. By variable-temperature NMR studies, these adducts were shown to be quite labile and this aspect is reflected in the reactivity of the hydride dimers with a variety of simple substrates. On the other hand, solution NMR experiments also show that the interaction is qualitatively quite strong since no evidence for dissociation of the adducts was found. In trying to gauge what promotes such an interaction, a number of features deserve mention: (a) the solution structures of the lithium and sodium tetraalkylborates (and aluminates) are not known; however, one might predict that the cation is labile and is involved in oligomeric aggregates; and (b) the palladium hydride dimer itself has very electron-rich metal centers [formally d^9 for each Pd(I)] and bridging hydrides, both sources of electron density for an ion–dipole type interaction with soluble alkali metal cations. Taken together, it is not unreasonable to predict that other electron-rich metal complexes with and without hydrides should show adduct formation with species such as $LiBEt_4$ and $NaBEt_4$. Such studies are currently in progress.

Acknowledgment. Financial support was provided by the donors of the Petroleum Research Fund, administered by the American Chemical Society. We also thank Johnson-Matthey for the generous loan of palladium salts.

Supplementary Material Available: Final atomic coordinates and equivalent isotropic thermal parameters, complete tables of bond lengths and angles, hydrogen atom parameters, anisotropic thermal parameters, torsion angles, intermolecular contacts, and least-squares planes for **1**, **2**, and **3** (110 pages); listing of measured and calculated structure factor amplitudes for **1**, **2**, and **3** (118 pages). This material is contained in many libraries on microfiche, immediately follows this article in the microfilm version of the journal, and can be ordered from the ACS; see any current masthead page for ordering information.

(47) Tebbe, F. N.; Parshall, G. W.; Reddy, G. S. *J. Am. Chem. Soc.* **1978**, *100*, 3611.

(48) Eisch, J. J.; Piotrowski, A. M.; Brownstein, S. K.; Gabe, E. J.; Lee, F. L. *J. Am. Chem. Soc.* **1985**, *107*, 7219.